MECHANICS OF COHESIVE-FRICTIONAL MATERIALS
Mech. Cohes.-Frict. Mater. **4**, 443–460 (1999)

An internal length scale in dynamic strain localization of multiphase porous media

H. W. Zhang[1]*, L. Sanavia[2] and B. A. Schrefler[2]

[1] *Research Institute of Engineering Mechanics, State Key Laboratory of Structural Analysis and Industrial Equipment, Department of Engineering Mechanics, Dalian University of Technology, 116024 Dalian, People's Republic of China*
[2] *Dipartimento di Costruzioni e Trasporti, Università degli Studi di Padova, 35131 Padova, Italy*

SUMMARY

In this paper, a length scale included in multiphase materials such as saturated and partially saturated porous media is discussed, where the viscous terms are introduced naturally by the fluid mass balance equations. The discussion is limited to the dynamic case. The characteristic stability equation is given in explicit form for one-dimensional wave propagation. It is shown that for axial waves a wave number domain exists for which the material model is dispersive when softening behaviour occurs for solid skeleton and that an internal length scale can be derived, while for ideal shear propagation this is not the case. Numerical examples are given to corroborate the validity of the expressions derived. Copyright © 1999 John Wiley & Sons, Ltd.

KEY WORDS: multiphase materials; stability analysis; strain softening; strain localization; internal length scale

1. INTRODUCTION

Strain localization and related material instability phenomena are of considerable interest because of their importance in failure prediction of materials. For isothermal rate-independent solids, strain localization has been analysed as a material instability within a theoretical framework due to Hadamard,[1] Thomas,[2] Hill[3] and Rice.[4] However, the employed material models do not involve a length-scale parameter, and related numerical solutions show an excessive mesh dependence. Recent studies[5,6] have elucidated the mathematical background of the mesh-sensitivity problem. The differential equation of motion ceases to be hyperbolic in some part of the domain as soon as softening occurs. The waves have there imaginary speed and are not able to propagate.[7] Consequently, the localization zones stay confined to lines or surfaces of zero thickness. This is against experimental evidence. The finite element solutions try to capture the localization zone of zero thickness, which results in their mesh dependence (see e.g. Reference 7).

Various kinds of modifications and generalizations of standard continuum plasticity have been proposed to avoid these difficulties in localization simulation such as viscoplasticity and gradient models (see e.g. Reference 8 for a review). Viscoplasticity has been recognized by several authors to provide a satisfactory framework for the analysis of dynamic strain localization in solids. As indicated in References 7, 9–13, rate-dependence naturally introduces a length-scale parameter into the dynamic initial value problem, even though the constitutive equations do not contain

* Correspondence to: H. W. Zhang, Research Institute of Engineering Mechanics, State Key Laboratory of Structural Analysis and Industrial Equipment. Department of Engineering Mechanics, Dalian University of Technology, 116024 Dalian, People's Republic of China.

CCC 1082-5010/99/050443–18$17.50

Received 19 September 1997
Revised 15 April 1998

a material parameter with the dimension of length. Gradient models possess a length scale and the obtained numerical results of localization problems are mesh independent (see e.g. Reference 8).

Strain localization in multiphase media has received less attention than in single phase materials. An internal length scale for multiphase materials is still not defined to the authors' knowledge. In the recent past, an enrichment to the porous media model has been introduced by Loret and Prevost[14] who included viscosity into the constitutive equation of the solid skeleton to regularize the porous media model under dynamic loading.

Numerical simulations of strain localization in a multiphase medium (i.e. fluid saturated geomaterials) have evidenced that the mesh dependence of the results is not so dramatic as in single phase materials.[15,16] Whereas in single phase materials, both the effective plastic strain and the band width are strongly mesh dependent unless some regularization is introduced,[7] in multiphase materials the equivalent plastic strain is mesh insensitive while the shear band width remains still dependent on the mesh size.[16]

The above difference between single and multiphase materials was attributed in Reference 16 to the natural presence of a gradient term in the mass balance equation of the fluid, through Darcy's law (linear momentum balance equation of the fluids) and the related constitutive relationship for permeability. The presence of the Laplace's operator and the numerical results presented in References 15 and 16 suggested that the used multiphase material model could contain an internal length scale.

The goal of this paper is to derive analytically this internal length for localization analysis in multiphase materials under dynamic loading conditions and to check the correspondence between the analytical length scale found and the finite elements results of the strain localization problem.

Strain localization in multiphase materials is a challenging and difficult topic because it is influenced both from a local and a structural aspect: the local aspect is given by the material behaviour and the structural aspect by the fluid–solid interaction. Hence, an internal length scale should be related to both of them.

In this paper the existence of a domain of parameters will be shown for which the one-dimensional governing equations of a multiphase material, with softening behaviour of the solid phase, do not loose their hyperbolicity on the onset of strain softening and admit a solution with real wave speed in case of axial waves. For this case an internal length parameter is defined. For ideal shear wave propagation the same results as in Reference 4 are then obtained where it has been shown that the multiphase material behaves like a single phase one and, without some sort of regularization, no internal length scale exists.

First the stability of such a multiphase material using standard linear stability analysis is investigated. This method considers the solution of exponential disturbances and permits to detect singularities which originate from the non-linearities of the governing equations. Within this method the Routh–Hurwitz criterion is used to determine whether the growth rate of the disturbance is positive or negative. Then the dispersive behaviour of the multiphase model is investigated when the solid skeleton is in the softening range. Finally, a length scale is computed in the way as done by Sluys[7] for rate-dependent single-phase materials.

The above length scale depends on several material parameters and in particular on the permeability. The influence of the permeability on the width of the shear band through the internal length scale is investigated numerically for a one-dimensional and a two-dimensional case and the results are presented in the last part of this paper.

2. GOVERNING EQUATIONS OF MULTIPHASE POROUS MEDIA

For fully or partially saturated porous media the following simplified equations hold, by assuming that the air phase remains at constant pressure in the partially saturated zone:[17,18]

$$\begin{aligned} \sigma'_{ij,j} - \bar{\alpha} S_w p_{,i} - \rho \ddot{u}_i &= 0 \\ -\dot{w}_i &= k p_{,i} \\ Q^*(\bar{\alpha} S_w \dot{u}_{i,i} + \dot{w}_{i,i}) + \dot{p} &= 0 \end{aligned} \tag{1}$$

where $\sigma'_{ij} = \sigma_{ij} + \bar{\alpha}\delta_{ij} S_w p$ is the modified effective stress (Bishop's stress), σ_{ij} the total stress, u_i the displacement of solid skeleton, S_w the water saturation, $\dot{w}$ the average water velocity relative to the solid phase, p the water pressure, $\bar{\alpha}$ Biot's constant, k the dynamic permeability is a function of S_w through the relative permeability parameter (see e.g. Reference 16) and the parameter Q^* is

$$Q^* = \left[\frac{n \partial S_w}{\partial p} + \frac{n S_w}{K_w} + \frac{S_w(\bar{\alpha} - n)}{K_s} \left(S_w + \frac{\partial S_w}{\partial p} p \right) \right]^{-1}$$

with K_s, K_w bulk moduli of the solid and water phases, respectively, and n the porosity.

From Reference 19 it can be shown that $k = k/\mu = k_w/\rho_w g$, where ρ_w is the water density, g the gravity acceleration, k_w the hydraulic conductivity ($[LT^{-1}]$), k the intrinsic permeability ($[L^2]$) and μ the dynamic viscosity.

The first equation of (1) is the linear momentum balance equation for the multiphase medium, the second one the linear momentum balance equation for water (Darcy's equation) and the third one the mass balance equation for water. The simplified equations neglect the effects of gravity (horizontal bar) and the convective term.

By introducing in these equations the absolute velocity of the fluid phase, $\dot{U}_i$, as:

$$\dot{U}_i = \dot{u}_i + \frac{\dot{w}_i}{n S_w} \tag{2}$$

the u–U form of the governing equations can be obtained:

$$\begin{aligned} \sigma'_{ij,j} + \bar{\alpha} n S_w^2 k^{-1}(\dot{U}_i - \dot{u}_i) - \rho \ddot{u}_i &= 0 \\ -Q^* k((\bar{\alpha} - n)\dot{u}_{j,j} + n\dot{U}_{j,j})_{,i} + n(\dot{U}_i - \ddot{u}_i) &= 0 \end{aligned} \tag{3}$$

We investigate wave propagation by considering the set of equations for a one-dimensional horizontal soil bar. The problem described by equation (3) will be divided into two cases: compressive wave and ideal shear wave propagation problems.

Hence equation (3) can respectively be divided into the following forms:

For compressive wave (u_x, $U_x \neq 0$, $u_y = U_y = u_z = U_z = 0$):

$$\begin{aligned} \sigma'_{xx,x} + \bar{\alpha} n S_w^2 k^{-1}(\dot{U}_x - \dot{u}_x) - \rho \ddot{u}_x &= 0 \\ -Q^* k \left((\bar{\alpha} - n) \frac{\partial^2 \dot{u}_x}{\partial x^2} + n \frac{\partial^2 \dot{U}_x}{\partial x^2} \right) + n(\dot{U}_x - \ddot{u}_x) &= 0 \end{aligned} \tag{4}$$

For ideal shear wave (u_y, $U_y \neq 0$, $u_x = U_x = u_z = U_z = 0$):

$$\begin{aligned} \sigma'_{xy,x} + \bar{\alpha} n S_w^2 k^{-1}(\dot{U}_y - \dot{u}_y) - \rho \ddot{u}_y &= 0 \\ n(\dot{U}_y - \ddot{u}_y) &= 0 \end{aligned} \tag{5}$$

It should be noted that equation (5) can be obtained by setting $Q^* = 0$ in equation (4). Hence, we will just pay attention to the compressive wave propagation analysis from which the results for ideal shear wave situation are easy to obtain.

3. CHARACTERISTIC EQUATION OF THE PROBLEM

We carry out a dispersion analysis for a one-dimensional soil bar, and consider the general solution for a single harmonic wave propagating through this soil bar with a displacement field of the form:

$$\begin{Bmatrix} \mathrm{d}u \\ \mathrm{d}U \end{Bmatrix} = \begin{Bmatrix} A_u \\ A_U \end{Bmatrix} \mathrm{e}^{\mathrm{i}(Kx-\omega t)} = A\mathrm{e}^{\mathrm{i}Kx+\varsigma t}, \quad \varsigma = -\mathrm{i}\omega \tag{6}$$

where ω is the angular frequency and K the wave number, starting from a state of fully homogeneous deformations.

For the (linear) dispersion analysis we consider the linear comparison solid of Hill[20] assuming that the stress–strain relationship of the solid skeleton is established directly by the softening modulus $\mathrm{d}\sigma' = h\,\mathrm{d}\varepsilon$, and that the condition $-\bar{\alpha}^2 S_{\mathrm{w}}^2 Q^* < h$ always holds.

Substituting equation (6) into equation (4), gives:

$$\begin{aligned} -hK^2 A_u + \bar{\alpha} n S_{\mathrm{w}}^2 k^{-1} \varsigma (A_U - A_u) - \rho \varsigma^2 A_u = 0 \\ Q^* k((\bar{\alpha} - n) K^2 \varsigma A_u + nK^2 \varsigma A_U) + n\varsigma^2 (A_U - A_u) = 0 \end{aligned} \tag{7}$$

The characteristic/determinant equation of eigenvalues is

$$\begin{vmatrix} -hK^2 - \bar{\alpha} n S_{\mathrm{w}}^2 k^{-1} \varsigma - \rho \varsigma^2 & \bar{\alpha} n S_{\mathrm{w}}^2 k^{-1} \varsigma \\ Q^* k(\bar{\alpha} - n) K^2 \varsigma - n\varsigma^2 & Q^* k n K^2 \varsigma + n\varsigma^2 \end{vmatrix} = 0 \tag{8}$$

and the following equation is obtained:

$$n\varsigma(\rho\varsigma^3 + \rho Q^* k K^2 \varsigma^2 + (hK^2 + \bar{\alpha}^2 S_{\mathrm{w}}^2 K^2 Q^*)\varsigma + kK^4 h Q^*) = 0 \tag{9}$$

Since $n \neq 0$, and the solution $\zeta = 0$ of equation (9) is obtained from the first order rate form of equation (3b), the characteristic equation for eigenvalue ς is

$$D(\varsigma) = b_0 \varsigma^3 + b_1 \varsigma^2 + b_2 \varsigma^1 + b_3 = 0 \tag{10}$$

where

$$b_0 = \rho, \qquad b_1 = \rho Q^* k K^2,$$

$$b_2 = K^2 h + \bar{\alpha}^2 S_{\mathrm{w}}^2 K^2 Q^*, \qquad b_3 = kK^4 h Q^*$$

4. STABILITY ANALYSIS

To study the stability of the problem, we use the Routh–Hurwitz criterion to determine if there are positive real parts in the roots of the polynomial equation (10). A necessary and sufficient

condition for stability is that all the roots of equation (10) have negative real parts. This holds if and only if the coefficients of the characteristic polynomial (10) satisfy

$$\Delta_0 = b_0 > 0, \qquad \Delta_1 = b_1 > 0,$$
$$\Delta_2 = \begin{vmatrix} b_1 & b_3 \\ b_0 & b_2 \end{vmatrix} > 0, \quad \Delta_3 = b_3\Delta_2 > 0 \tag{11}$$

where

$$\Delta_0 = \rho, \qquad \Delta_1 = \rho Q^* K^2 k,$$
$$\Delta_2 = \rho\bar{\alpha}S_w^2 kK^4 Q^{*2}, \quad \Delta_3 = K^6 k^2 \rho h \bar{\alpha}^2 S_w^2 \tag{12}$$

The determinant conditions (11) always hold when the condition $h > 0$ is satisfied. For $-\bar{\alpha}^2 S_w^2 Q^* < h < 0$, loss of stability may appear as has been pointed out by several authors and a small perturbation can grow, for instance, into a shear band. In fact, when $-\bar{\alpha}^2 S_w^2 Q^* < h < 0$

$$D(0) < 0, \quad D(+\infty) > 0 \tag{13}$$

which means that there is always a positive real part in the root of equation (10). It appears also directly from the fourth of equation (12) that Δ_3 becomes negative.

The standard form of determinant equation (10) can be rewritten in the following cubic form:

$$\varsigma^3 + a\varsigma^2 + b\varsigma + c = 0 \tag{14}$$

where

$$\begin{aligned} a &= a^0 Ky, \quad a^0 = Q^* \\ b &= b^0 K^2, \quad b^0 = (h + \bar{\alpha}^2 S_w^2 Q^*)\rho^{-1} \\ c &= c^0 K^3 y, \quad c^0 = Q^* h \rho^{-1} \\ y &= kK \end{aligned} \tag{15}$$

There are two kinds of solutions of equation (14) under the condition: $-\bar{\alpha}^2 S_w Q^* < h < 0$. One has one real positive root and two conjugate complex roots. The other possibility is three real roots in which at least one is positive. The conditions for one or the other case to occur are expressed by the sign of the following polynomial Q built with the coefficients a, b, c of equation (14):

$$Q = \left(\frac{R}{3}\right)^3 + \left(\frac{q}{2}\right)^2, \quad R = -\frac{a^2}{3} + b, \quad q = 2\left(\frac{a}{3}\right)^3 - \frac{ab}{3} + c \tag{16}$$

where the case with one real and two complex conjugate roots is characterized by

$$Q > 0 \tag{17a}$$

while the case of the three real roots is characterized by

$$Q \leqslant 0 \tag{17b}$$

In the first case, equation (17a), the wave propagation is possible and hence the governing equations remain hyperbolic also when the solid skeleton is softening; the results from the finite element analysis will not present mesh sensitivity. On the contrary, when $Q \leqslant 0$, (equation (17b)),

the wave speed becomes imaginary and hence the dynamic governing equation becomes elliptic; the finite element analysis will present mesh dependence.

The three roots of equation (10) can be expressed as

$$\varsigma_1 = A + B - \frac{a}{3}, \qquad \varsigma_{2,3} = -\frac{a}{3} - \varsigma_r \pm i\varsigma_i \tag{18}$$

in which

$$\begin{aligned} A &= \sqrt[3]{-\frac{q}{2} + \sqrt{Q}}, \quad B = \sqrt[3]{-\frac{q}{2} + \sqrt{Q}} \\ \varsigma_r &= \frac{A+B}{2} + \frac{a}{3}, \qquad \varsigma_i = \frac{A-B}{2}\sqrt{3} \end{aligned} \tag{19}$$

Upon substitution of equations (15), (16b) and (16c) into equation (16a), the equality form of equation (16a) will be obtained as

$$Q(y) = wy^4 + ry^2 + s = 0 \tag{20}$$

in which the coefficients are

$$\begin{aligned} w &= \frac{1}{27}\, a^{0^3} c^0, \quad s = \frac{1}{27}\, b^{0^3}, \\ r &= \frac{1}{4}\, c^{0^2} - \frac{1}{6}\, a^0 b^0 c^0 - \frac{1}{108}\, a^{0^2} b^{0^2} \end{aligned} \tag{21}$$

It is easy to obtain the only positive root of equation (20):

$$y^2 = \frac{-r - \sqrt{r^2 - 4ws}}{2w} = y_0^2 \tag{22}$$

and the criterion in equation (17) then changes into (see the last of the equations (15), i.e. $y = kK$):

$$Q > 0 \Leftrightarrow K < \frac{y_0}{k}, \quad \text{one real and two complex conjugate roots} \tag{23a}$$

$$Q \leqslant 0 \Leftrightarrow K \geqslant \frac{y_0}{k}, \quad \text{three real roots} \tag{23b}$$

respectively. It is important to underline that the amplitude of the two regions depends on the material parameters h, E, n, ρ, α, Q^* and S_w.

Figure 1 shows the two regions identified by equations (17) or (23) for the following parameters: $Q^* = 20{\cdot}0$ MPa, $h = -5{\cdot}0$ MPa, $\rho = 2000$ kg/m^3, $\bar{\alpha} = 1{\cdot}0$, $S_w = 1{\cdot}0$. The value of y_0 calculated is equal to $0{\cdot}11009\mathrm{E}-04$ m.

Remark 1: dispersion analysis

Following the idea developed in reference 7 the dispersion analysis appears to be important in localization problems in order to check the ability of a material model to capture localization phenomena. A medium is called dispersive when the phase velocity $c_w = \omega/K$ is a function of

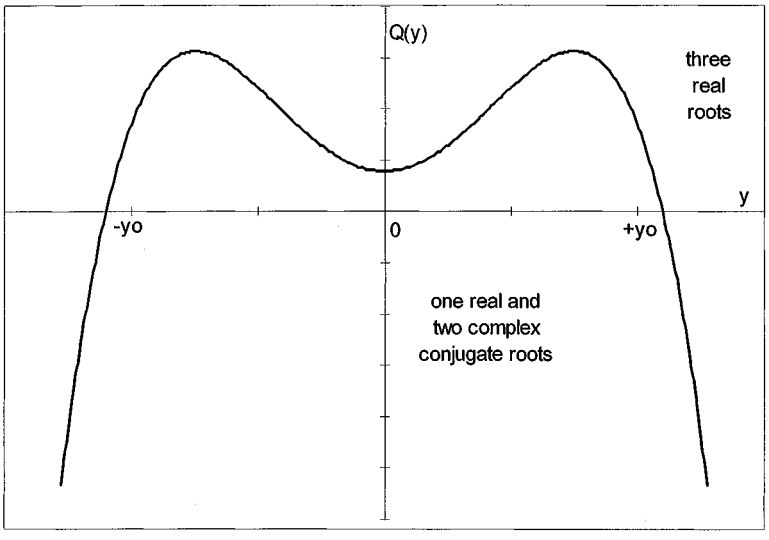

Figure 1. Distribution of the two regions identified by equation (23) for partially and fully saturated geomaterials

a wave number K; this allows the model to describe adequately the localization zone because it is able to change the shape of a loading wave into a stationary wave representing the localization zone.[7]

For multiphase materials ω is related to the imaginary part ζ_i of ζ. The phase velocity c_f is hence $c_w = |\zeta_i|/K$, where ζ_i is given by equation (19).

From equations (19), (16) and (15) it can be shown that c_w is a function of the wave number K and the permeability k. For elastic material, ζ_i always exists and the material is dispersive, as pointed out by Biot.[21] In case of elasto-plastic solid skeleton with softening, the multiphase material will be either dispersive or non-dispersive depending on the wave number K. In fact when K is smaller than y_0/k, the material is dispersive, while with K greater or equal than y_0/k, i.e. when the wave speed is imaginary, the multiphase material is not dispersive. The dispersion relation ω–K is depicted in Figure 2.

5. INTERNAL LENGTH SCALE PREDICTION

The length scale value naturally generated by the seepage permeability in fully and partially saturated porous media will depend on the complex roots of equation (10), because there we have a solution with real wave speed.

Substituting the complex root equation (18) into equation (6), we have

$$v(x,t) = A e^{iKx} e^{-(\varsigma_r + (a/3))t - i\varsigma_i t}, \quad v = [u, U]^T \tag{24}$$

Recalling the relation between wave (phase) speed c_w and wave number K:

$$c_w = \frac{|\varsigma_i|}{K} \tag{25}$$

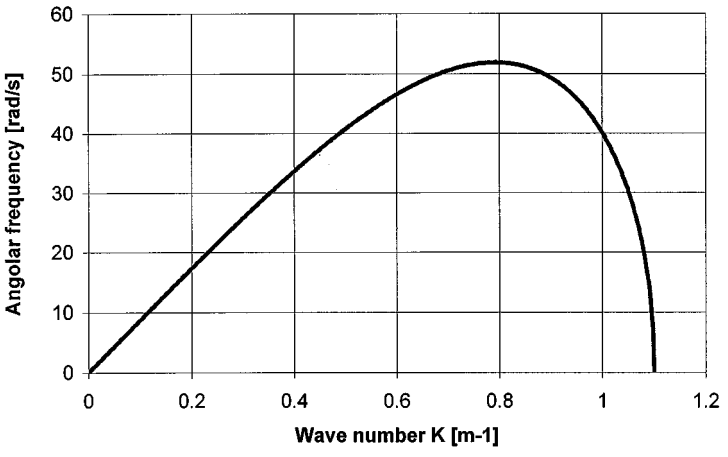

Figure 2. Dispersion relation ω–K for multiphase material with elasto-plastic solid skeleton in softening

Then by means of $t = x/c_w$, the damping term $\exp[-(\varsigma_r + (a/3))t]$ in equation (24) changes into $\exp[-K((\varsigma_r + (a/3))/|\varsigma_i|)x] = e^{-\alpha x}$, where α is the damping coefficient.

We remind that the presence of the fluid introduces a rate dependent overall behaviour, even if the solid phase itself presents only softening. For the multiphase medium we introduce hence a length scale in the way as it was done by Sluys[7] for rate-dependent single-phase materials. Actually, the characteristic dispersion equations have the same structure for these two cases. This internal length l is hence

$$l = \alpha^{-1}, \qquad \alpha = \frac{\varsigma_r + (a/3)}{|\varsigma_i|}K \tag{26}$$

in which ς_r and ς_i are obtained from equation (19). It is obvious that the above length scale definition holds only for dynamic analysis.

Unlike the rate-dependent single-phase materials[22] we have here $Q > 0$ when $0 < K < y_0/k$. When $K \geqslant y_0/k$, there are only real roots for equation (10), and the problem will present mesh sensitivity. This situation may arise when the permeability value is very large. When $K < y_0/k$, the internal length can be obtained from equation (26) in the region $[K, y_0/k]$. When permeability is very small, the internal length may be larger than the maximum size of the structure geometry. In this case, the localization zone will disperse throughout the whole structure as shown by the second example.

Remark 2: wave number domain

When the size of the structure is considered, there exists a lower limit for the wave number K. In fact the maximum wave length that can propagate in a bar with length L is $2L$ and hence $K_{min} = \pi/L$. If $K_{min} > y_0/k$, no waves can propagate in the softening zone and hence the numerical problem will be mesh dependent.

The wave number of domain for which the governing equation remains hyperbolic when the solid skeleton is in the softening range is hence: $\pi/L \leqslant K < y_0/k$.

Since the seepage permeability is generally small, we can obtain for practical purposes the approximate length scale predicted by means of equation (26) with respect to small permeability. From (15) and (16), we have

$$-\frac{q}{2} = a_1 k + a_2 k^3 \tag{27}$$

$$Q = a_3 + a_4 k^2 + a_5 k^4 \tag{28}$$

where

$$a_1 = \left(\frac{E_2 - 3h}{6}\right)\frac{Q^* K^4}{\rho}, \qquad a_2 = -\frac{1}{27}\frac{Q^{*3} K^6}{m^3}, \qquad a_3 = \frac{E_2^3 K^6}{27\rho^3}, \tag{29}$$

$$a_4 = \left(\frac{c_0^2}{4} - \frac{a_0 b_0 c_0}{6} - \frac{a_0^2 b_0^2}{108}\right)K^8, \qquad a_5 = \frac{a_0^3 c_0 K^{10}}{27}, \quad E_2 = \bar{\alpha}^2 S_w^2 Q^* + h \tag{30}$$

With the use of equation (19), the damping coefficient α of equation (26) can then be expressed as

$$\alpha = \frac{|A + B|K}{(A - B)\sqrt{3}} = \frac{K\left|\sqrt[3]{-\frac{q}{2} + \sqrt{Q}} + \sqrt[3]{-\frac{q}{2} - \sqrt{Q}} + \frac{2a}{3}\right|}{\sqrt{3}\left(\sqrt[3]{-\frac{q}{2} + \sqrt{Q}} - \sqrt[3]{-\frac{q}{2} - \sqrt{Q}}\right)}$$

$$= \frac{K\left|\sqrt[3]{a_1 k + a_2 k^3 + \sqrt{a_3 + a_4 k^2 + a_5 k^4}} + \sqrt[3]{a_1 k + a_2 k^3 - \sqrt{a_3 + a_4 k^2 + a_5 k^4}} + \frac{2}{3} a_0 k K^2\right|}{\sqrt{3}\left(\sqrt[3]{a_1 k + a_2 k^3 + \sqrt{a_3 + a_4 k^2 + a_5 k^4}} - \sqrt[3]{a_1 k + a_2 k^3 - \sqrt{a_3 + a_4 k^2 + a_5 k^4}}\right)}$$

The limit form of equation (31) with respect to a small value of k is

$$\alpha \cong \frac{K|(a_1 k/\sqrt{a_3}) + (a_0 k K^2/\sqrt[6]{a_3})|}{3\sqrt{3}} \tag{32}$$

Consequently, by means of substitution of equations (29) and (30) into equation (32), the approximate values for α and l (equation (26)) are determined as

$$\alpha \cong \frac{k K^2 \bar{\alpha}^2 S_w^2 Q^*}{2 c_m \eta}, \qquad l \cong \frac{2 c_m \eta}{k K^2 \bar{\alpha}^2 S_w^2 Q^*} \tag{33}$$

with

$$c_m = \sqrt{\frac{E_2}{\rho}}, \qquad \eta = \frac{E_2}{Q^*} \tag{34}$$

When E_2 is equal to zero, from equation (30c) the hardening value h is equal to $-\bar{\alpha}^2 S_w^2 Q^*$. This is a critical value for h because below this value, i.e. when the parameter E_2 is less than zero, the velocity c_m is imaginary, the length scale l disappears and the finite element results are mesh dependent.

Equation (33) holds under the condition of small permeability and not too large Q^*. In equation (33) c_m can be understood as the wave speed of the volume fraction mixture under undrained conditions.

Remark 3

The length scale (33b) is dependent on some material parameters (known) and on the wave number K, which has to be computed. We assume that this internal length will be set by the wave number of the first (plastic) wave for which the shear band will start to form; in fact the wave number of the successive waves is larger and hence the internal length associated to these waves is smaller.

If K is unknown, we can estimate the length scale l by choosing a value for K. E.g. for $K = 1$, equation (34) reads

$$\alpha \propto \frac{k\bar{\alpha}^2 S_w^2 Q^*}{2c_m \eta}, \quad l \propto \frac{2c_m \eta}{k\bar{\alpha}^2 S_w^2 Q^*} \tag{35}$$

which may be used as estimates of l (and α) if K is not known.

Finally, for the ideal shear wave propagation problems, we set $Q^* = 0$ and then equation (10) reduces to

$$D(\varsigma) = \varsigma(\rho\varsigma^2 + K^2 h) = 0 \tag{36}$$

Obviously, for ideal shear wave propagation, the permeability will no longer play the role of a length scale parameter for strain localization analysis, at least in one-dimensional problems.

6. LIMIT STATE: INCOMPRESSIBLE FLUID

To investigate the limit state of compressive wave propagation when the fluid in porous media is incompressible, i.e. $Q^* \to \infty$, two cases are discussed in what follows:

Case 1. $Q^* \to \infty$, permeability k and wave number K are finite values.

In this case, from equation (20), we get

$$Q = c_4 Q^{*4} + c_3 Q^{*3} + c_2 Q^{*2} + c_1 Q^* + c_0 \tag{37}$$

When $Q^* \to \infty$, the control parameter of equation (37) will mainly depend on the coefficient c_4, whose explicit form is

$$c_4 = \frac{hk^4 K^{10}}{27\rho} - \frac{\bar{\alpha}^4 S_w^4 k^2 K^8}{108\rho^2} \tag{38}$$

Obviously, $c_4 < 0$ always holds when $h < 0$, therefore in this case the characteristic equation (10) has three real roots, and no internal length parameter exists. In fact, when $Q^* \to \infty$, the characteristic equation (10) will change into

$$D(\varsigma) = a'\varsigma^2 + b'\varsigma^1 + c' = 0 \tag{39}$$

where

$$a' = \rho k K^2, \qquad b' = \bar{\alpha}^2 S_w^2 K^2, \qquad c' = kK^4 h \tag{40}$$

It is easy to prove that $b'^2 - 4a'c' > 0$ holds when $h < 0$, which confirms the above conclusion.

Case 2. $Q^* \to \infty$, permeability $k = 0$ (undrained case) and wave number K is finite.
In this case the characteristic equation (10) reduces to

$$D(\varsigma) = \varsigma(\rho\varsigma^2 + \bar{\alpha}^2 S_w^2 K^2 Q^* + K^2 h) = \varsigma(\rho\varsigma^2 + K^2 E_2) = 0 \tag{41}$$

It is clear that in this case two pure complex conjugate roots are obtained and the internal length scale will tend to be infinite.

These two cases are now shown to be limiting situations of expression (35) obtained in the previous section. For case 1, when permeability k and wave number K are finite values, when Q^* is infinite, the length scale will be proportional to $1/\sqrt{Q^*}$ and hence it tends to zero. In fact introducing equations (34) and (30c) in equation (33b) one can obtain:

$$l \propto \frac{2\bar{\alpha} S_w}{kK^2\sqrt{\rho}} \frac{1}{\sqrt{Q^*}} \tag{42}$$

For case 2 we assume, without loss of generality, $Q^* = \beta/k$ where β is a factor with a finite value. When the permeability k is infinitely small, the internal length scale will be proportional to $1/\sqrt{k}$, and tends to be infinite.

7. NUMERICAL ILLUSTRATION

To illustrate the influence of the permeability on the width of the localization zone a one- and a two-dimensional soil domain has been investigated using a dynamic finite element code. In the first case, the mesh independence of the plastic zone has also been shown, while in the second case some numerical results obtained by Schrefler and co-workers [14] has been explained.

Example 1

A one-dimensional soil bar under axial compressive deformation is investigated numerically. The geometrical, material and loading data for the soil bar are given in Figure 3. The left surface is open

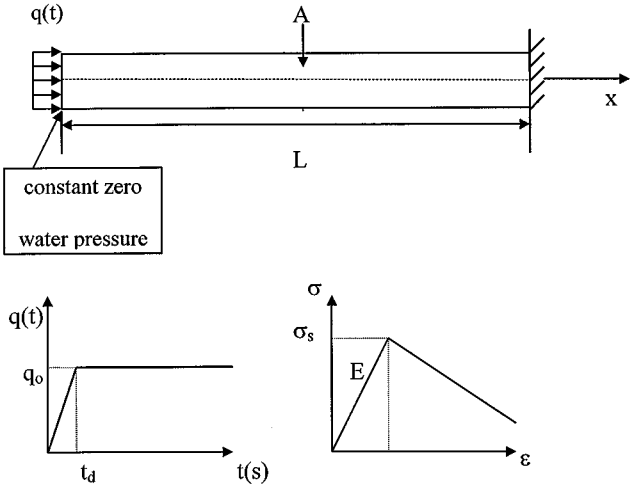

Figure 3. One-dimensional soil bar in axial compression

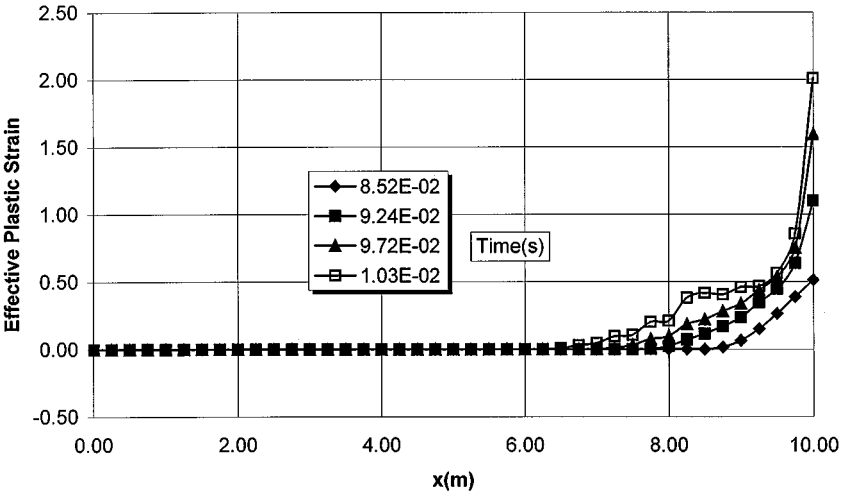

Figure 4. Development of the localization zone when $k_w = 1{\cdot}0\text{E} - 02$ m/s and $\sigma_s = 1{\cdot}1$ MPa

to flow, while the others are impervious. The domain is discretized by means of 40 isoparametric quadrilateral bilinear finite elements. The solid and fluid domains are not subject to any initial stress state (hence gravitational effects or hydrostatic pressures are not accounted for). The reduced von Mises plasticity model used in this region has the form:

$$f = |\sigma_{xx}| - \sigma_s - h\lambda \tag{43}$$

To illustrate the influences of the permeability, three permeability values $k_w = 1{\cdot}0\text{E} - 0{\cdot}2$, $k_w = 1{\cdot}0\text{E} - 01$ and $k_w = 5{\cdot}0\text{E} - 01$ m/s are selected, respectively, in the following simulations. Equations (33) are then

$$\alpha \cong \frac{kK^2}{0{\cdot}065\text{E} - 04}\,\text{m}^{-1}, \qquad l \cong \frac{0{\cdot}065\text{E} - 04}{kK^2}\,\text{m} \tag{44}$$

and l is

k_w (m/s)	k (m^3 s/kg)	l ($K = 1$) (m)
$1{\cdot}0\text{E} - 02$	$1{\cdot}0\text{E} - 06$	6·50
$1{\cdot}0\text{E} - 01$	$1{\cdot}0\text{E} - 05$	0·65
$5{\cdot}0\text{E} - 01$	$5{\cdot}0\text{E} - 05$	0·13

The development of the localized zone of the three cases is shown in Figures 4–6, respectively. These three figures show the increase of the plastic zone when permeability decreases,[5] highlighting the sensitivity of the plastic zone to the permeability value as predicted by the analytical expression of the length scale, equation (33).

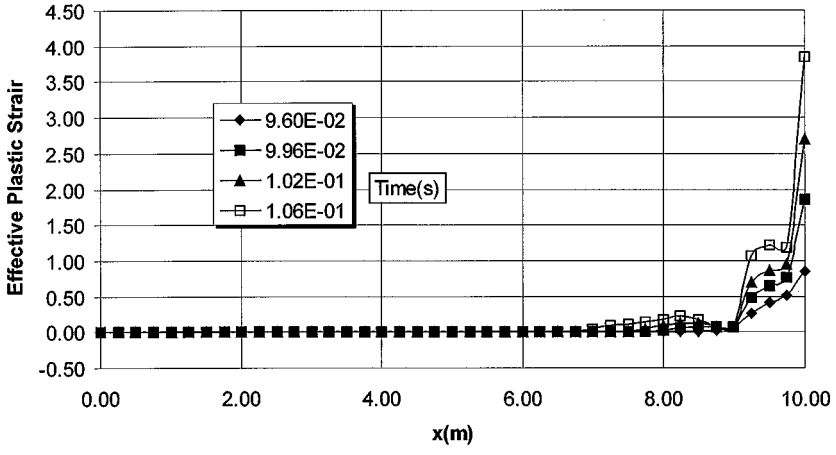

Figure 5. Development of the localization zone when $k_w = 1{\cdot}0E - 1$ m/s and $\sigma_s = 1{\cdot}1$ MPa

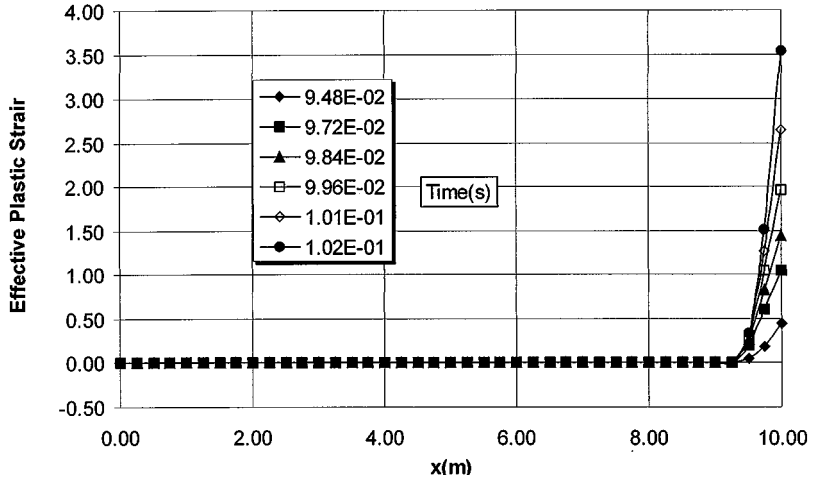

Figure 6. Development of the localization zone when $k_w = 5{\cdot}0E - 01$ m/s and $\sigma_s = 1{\cdot}4$ MPa

Moreover, these figures show that in the first two cases the plastic wave is able to propagate, while in the third case not because of the large permeability value and the very small wave number domain $K < y_0/k = 0{\cdot}22\ \mathrm{m}^{-1}$ where the equations remain hyperbolic. In fact, in this case, the $K_{\min}$ of Remark 2 is equal to $0.31\ \mathrm{m}^{-1}$.

Because the water pressure will decrease when k is increased, the initial yield stress in Figure 6 is increased to ensure that the initial softening plastic zone will start at the right side of the soil bar.

The one-dimensional case of Figure 3 has also been solved using three different meshes: 10, 20 and 40 f.e. A permeability value of $1{\cdot}0E - 02$ m/s has been used. The equivalent plastic strain distribution along the bar has been plotted in Figure 7, where the independence of the shear band width from the finite element dimension is shown.

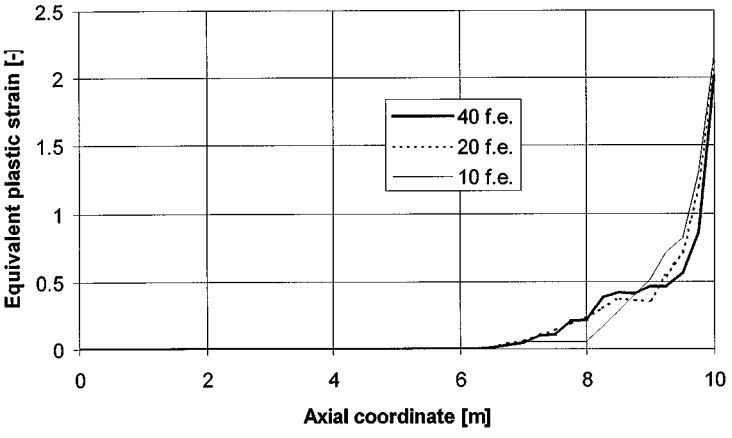

Figure 7. Equivalent plastic strain distributed along the bar using three different meshes (10, 20 and 40 f.e.)

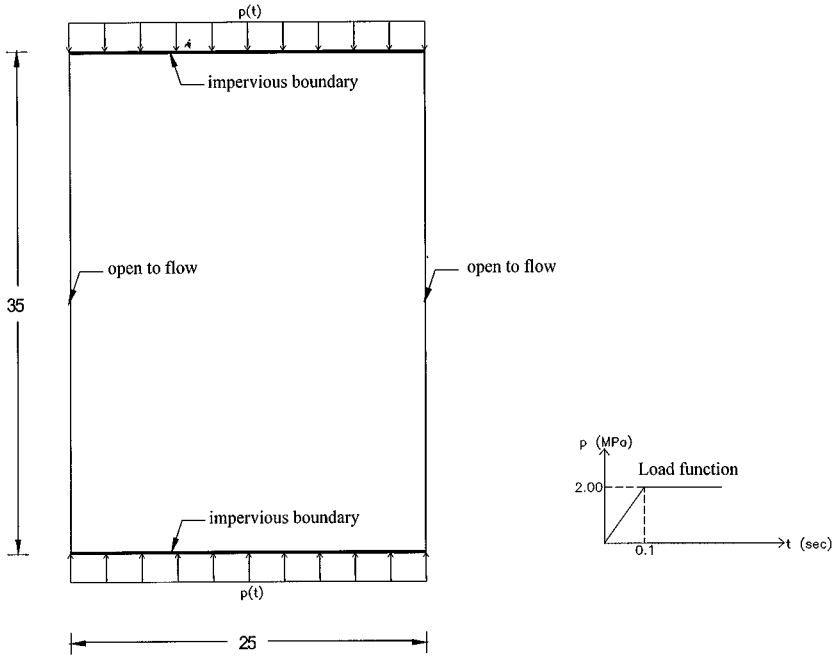

Figure 8. Description of the geometrical and material characteristics of the second example

Example 2

The cross section of a geological formation, shown in Figure 8, is investigated as the second numerical example. Such a section was first analysed by Loret and Prevost[14] and then by Schrefler *et al.*[15] The sample is subject to axial compression by means of uniformly distributed loads both on the upper and lower surfaces, as also indicated in Figure 8.

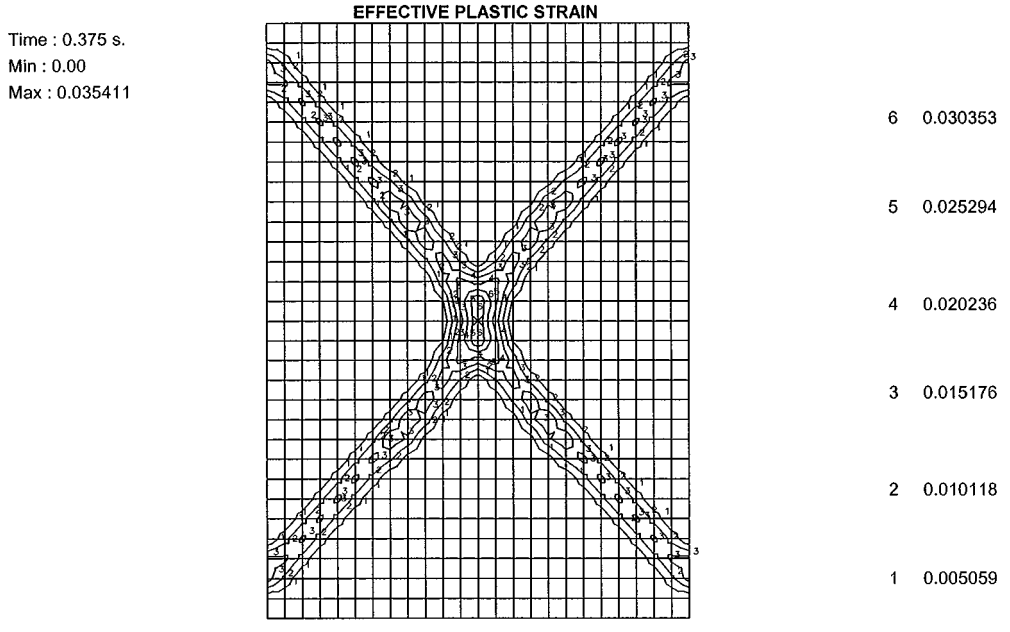

Figure 9. Effective plastic strain at $t = 0{\cdot}375$ s with a permeability of 0·25 m/s

The top and bottom surfaces are considered impermeable. As in the one-dimensional case the solid and fluid domains are not subject to any initial stress state and the domain is discretized by means of 720 isoparametric quadrilateral bilinear finite elements.

In the considered model, homogeneous and isotropic solid and fluid phases are assumed. A Mohr–Coulomb yield criterion with associative flow rule and isotropic linear cohesion softening is used for the solid skeleton. Plane strain condition is assumed.

Permeability affects the degree of coupling between the two phases and presents a significant role in the development of localization. From a physical point of view the lower is its value, the higher is the part of the load increment assumed by water and the slower is the transfer to the solid skeleton; compare for instance the maximum value of the effective plastic strain (Figures 9–11). Hence coupling effects increase as the permeability decreases. If we use the length scale prediction given by equation (35) for the one-dimensional case, for permeability values of 0·25, 0·25E − 3 and 0·25E − 10 m/s, the length scale from equation (35) is 5·55E − 6, 5·55E − 3 and 5·55E + 4 m, respectively. From Figures 9–11 it appears that the plastic zone increases with the internal length up to spreading over the whole domain when the length scale assumes a very large value (Figure 11).

k_w (m/s)	k (m^3 s/kg)	l ($K = 1$) (m)
0·25	0·25E − 04	5·55E − 06
0·25E − 03	0·25E − 07	5·55E − 03
0·25E − 10	0·25E − 14	5·55E + 04

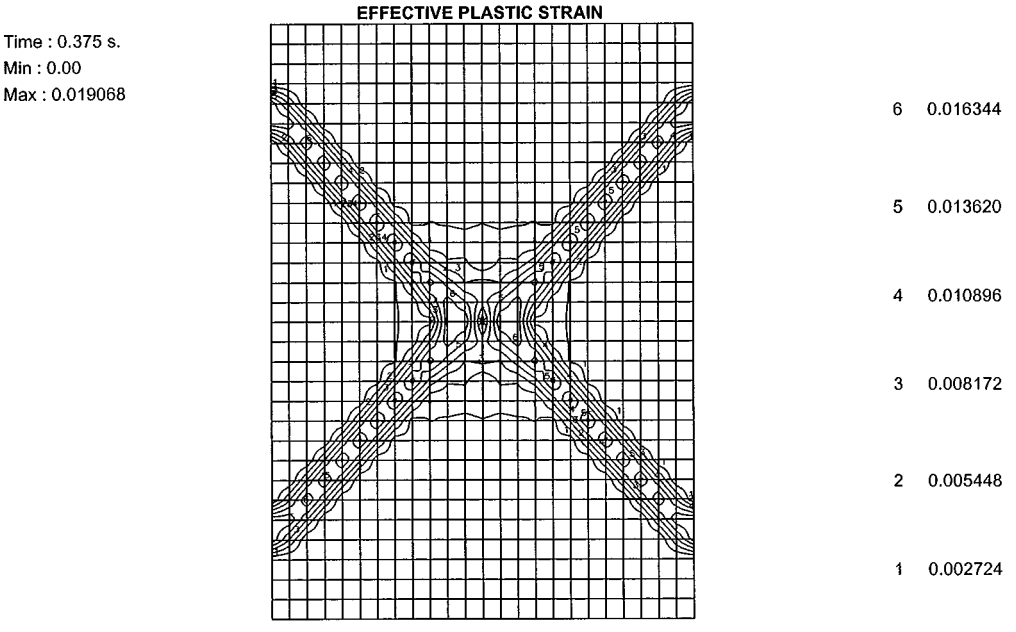

Figure 10. Effective plastic strains at $t = 0{\cdot}375$ s with a permeability of $0{\cdot}25\text{E} - 03$ m/s

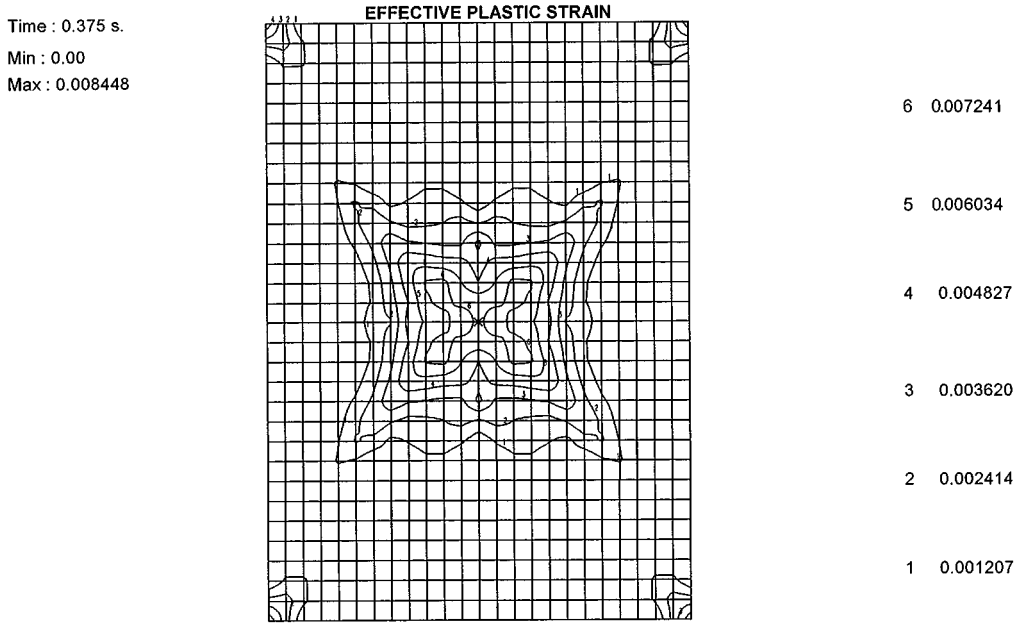

Figure 11. Effective plastic strains at $t = 0{\cdot}375$ s with a permeability of $0{\cdot}25\text{E} - 10$ m/s

The very small length scale value of the material in case of permeability of 0·25 m/s ($l_{(K=1)} = 5{\cdot}55\text{E} - 06$ m) could explain the dependence of the shear band width on the mesh size obtained in Reference 16 (Figures 18 and 19). In fact this value of l is much smaller than the dimension of the finite element used (≈ 1 m) and hence the band width can only be constrained in one element.

8. CONCLUSIONS

The one-dimensional wave propagation problem in partially and fully saturated porous media has been studied in this paper. It has been shown that for axial waves there exists a wave number domain for which the material model is dispersive when softening behaviour occurs for the solid skeleton. The length scale related to axial waves and included in the model where the viscous terms (drag force) are introduced naturally by the fluid mass balance equations, has been discussed. The length scale derived considers the contribution of the softening modulus and the permeability besides other material parameters such as elastic modulus, density of the medium, etc. It is very important to outline that the obtained length scale is linked to the microstructure of the medium (mean grain diameter d) e.g. via $k = 0{\cdot}617 \times 10^{-11}\, d^2$,[19] where k is the intrinsic permeability (k and d are expressed in cm^2 and μm).

It has been found that for very small permeability the internal length may be larger than the sample, with the localization zone spreading over the whole structure. Numerical results of one- and two-dimensional examples corroborate the conclusions obtained analytically. The mesh independence of the localization zone in the one-dimensional case has also been shown. No length scale has been found in the case of a shear wave propagation problem, as shown in Reference 4.

ACKNOWLEDGEMENTS

This work was supported by the EC International Scientific Co-operation Programme, the State Educational Committee and the National Natural Science Foundation of China and the Italian Ministry of Scientific and Technological Research (MURST 40%).

REFERENCES

1. J. Hadamard, *Lecons sur la Propagation des Ondes et les Equations de l'hydrodynamicque*, Librairie Scientifique A., Hermann, Paris, France, 1903 (in French).
2. Y. Thomas, *Plastic Flow and Fracture in Solids*, Academic Press, New York, 1961.
3. R. Hill, 'Acceleration waves in solids', *J. Mech. Phys. Solids*, **10**, 1–16 (1962).
4. J. R. Rice, 'On the stability of dilatant hardening for standard rock masses', *J. Geophys. Res.*, **80**, 1531–1536 (1975).
5. H. E. Read and G. A. Hegemier, 'Strain softening of rock, soil and concrete—A review article', *Mech. Mater.*, **3**, 271–294 (1984).
6. D. Lasry and T. B. Belytschko, 'Localisation limits in transient problems', *Int. J. Solids Struct.*, **24**, 581–597 (1988).
7. L. J. Sluys, 'Wave propagation, localisation and dispersion in softening solids', *Ph.D. thesis*, Department of Civil Engineering, Delft University of Civil Engineering, Netherlands.
8. R. de Borst, L. J. Sluys, H. B. Muhlhaus, J. Pamin, 'Fundamental issues in finite element analysis of localisation of deformation', *Engng. Comput.*, **10**, 99–121 (1993).
9. F. H. Wu and L. B. Freund, 'Deformation trapping due to thermoplastic instability in one-dimensional wave propagation', *J. Mech. Phys. Solids*, **32**, 119–132 (1984).
10. A. Needleman, 'Material rate dependence and mesh sensitivity on localisation problems', *Comput. Meth. Appl. Mech. Engng.*, **67**, 69–86 (1988).
11. R. J. Asaro, 'Mechanics of crystals and polycrystals', *Adv. Appl. Mech.*, **23**, 2–115 (1983).

12. B. Loret and J. H. Prevost, 'Dynamic strain localisation in elasto (visco-) plastic solids, Part 1. General formulation and one-dimensional examples', *Comput. Meth. Appl. Mech. Engng.*, **83**, 247–273 (1990).
13. L. J. Sluys and R. de Borst, 'Solution methods for localisation in fracture dynamics', in J. van Mire, J. G. Rots and A. Bakker, eds., *Proc. Conf. on Fracture Process in Concrete*, *Rock and Ceramics*, Chapman and Hall, London, 1991, pp. 661–671.
14. B. Loret and J. H. Prevost, 'Dynamic strain localisation in fluid—saturated porous media', *J. Engng. Mech.*, **11**, 907–922 (1991).
15. B. A. Schrefler, C. E. Majorana and L. Sanavia, 'Shear band localisation in saturated porous media', *Arch. Mech.*, **47**, 577–599 (1995).
16. B. A. Schrefler, L. Sanavia and C. E. Majorana, 'A multiphase medium model for localisation and post localisation simulation in geomaterials', *Mech. Cohesive-Frictional Mater. Struct.*, 95–114 (1996).
17. O. C. Zienkiewicz, Y. M. Xie, B. A. Schrefler, A. Ledesma and N. Bicanic, Static and dynamic behaviour of soils: a rational approach to quantitative solutions. II semi-saturated problems, *Proc. R. Sci. London A* **429**, 311–321 (1990).
18. B. A. Schrefler, 'F.E. in environmental engineering: Coupled thermo-hydromechanical process in porous media including pollutant transport', *Arch. Comput. Meth. Engng.*, **2**, 1–54 (1995).
19. J. Bear, *Dynamics of Fluid in Porous Media*, Dover, New York, 1972.
20. R. Hill, 'A general theory of uniqueness and stability in elastic–plastic solids', *J. Mech. Phys. Solids*, **6**, 236–249 (1958).
21. M. A. Biot, 'Theory of propagation of elastic waves in a fluid saturated porous solid, I. Low-frequency range, II. Higher frequency range', *J. Acoust. Soc. Am.*, **28**(2), 168–178, 179–191 (1956).
22. B. A. Schrefler, H. W. Zhang and L. Sanavia, Fluid–structure interaction in the localisation of saturated porous media, *ZAMM* (at press).

